

# Biomimetic Water-Responsive Self-Healing Epoxy with Tunable Properties

Dian Yuan,<sup>†</sup> Sébastien Delpierre,<sup>‡</sup> Kai Ke,<sup>\*,†</sup> Jean-Marie Raquez,<sup>\*,‡</sup> Philippe Dubois,<sup>‡</sup> and Ica Manas-Zloczower<sup>\*,†</sup>

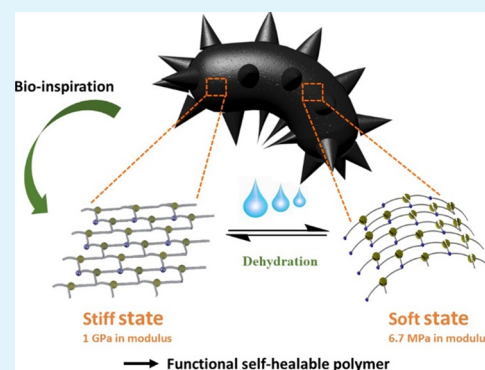
<sup>†</sup>Department of Macromolecular Science and Engineering, Case Western Reserve University, Cleveland, Ohio 44106, United States

<sup>‡</sup>Laboratory of Polymeric and Composite Materials (LPCM), Center of Innovation and Research in Materials and Polymers (CIRMAP), University of Mons, Place du Parc 23, 7000 Mons, Belgium

## Supporting Information

**ABSTRACT:** As dynamic cross-linking networks are intrinsically weaker than permanent covalent networks, it is a big challenge to obtain a stiff self-healing polymer using reversible networks. Inspired by the self-healable and mechanically adaptive nature of sea cucumber, we design a water-responsive self-healing polymer system with reversible and permanent covalent networks by cross-linking poly(propylene glycol) with boroxine and epoxy. This double cross-linked structure is self-healing due to the boroxine reversible network as well as showing a room-temperature tensile modulus of 1059 MPa and a tensile stress of 37 MPa, on a par with classic thermosets. The dynamic boroxine bonds provide the self-healing response and enable up to 80% recovery in modulus and tensile strength upon water contact. The system shows superior adhesion to metal substrates by comparison with the commercial epoxy-based structural adhesive. Besides, this system can change modulus from a stiff thermoset to soft rubber (by a factor of 150) upon water stimulus, enabling potential applications of either direct or transform printing for micro/nanofabrication. Moreover, by incorporating conductive nanofillers, it becomes feasible to fabricate self-healing and versatile strain/stress sensors based on a single thermoset, with potential applications in wearable electronics for human healthcare.

**KEYWORDS:** self-healing, water-responsive, epoxy, boroxine, strain sensors



## 1. INTRODUCTION

In recent decades, inspired by natural organisms, self-healing materials with the capability of repairing physical damages with or without external intervention are widely developed by material scientists.<sup>1,2</sup> Such functionality enables the extension of material's lifetime by restoring its performance upon damage thus reducing waste.<sup>3–6</sup> Based on the healing mechanism, self-healing materials can generally be divided into two categories: (i) intrinsic self-healing materials containing covalent or noncovalent reversible bonds<sup>7–11</sup> and (ii) extrinsic self-healing materials, which can release a healing agent or catalyst from dispersed microcapsules or microvascular networks.<sup>12,13</sup> Unlike extrinsic self-healing materials relying on the healing functionality from a secondary phase or additives, intrinsic self-healing materials are more desirable because they can retain good healing efficiency after multiple healing cycles based on reversible bonds.<sup>14,15</sup>

Due to the good combination of mechanical robustness and reversibility, dynamic covalent bonding using disulfide,<sup>16</sup> olefin metathesis,<sup>17</sup> radical reshuffling,<sup>9</sup> siloxane,<sup>18</sup> and Diels–Alder reactions<sup>19</sup> has been used to make intrinsically self-healing polymers. However, these materials are limited by complex chemistry and high-cost strategies to stimulate intrinsically self-

healing properties.<sup>20</sup> Among intrinsic self-healing materials, water-enabled self-healing polymer looks promising because the healing can be achieved by simply exposing materials to water or moisture. Strategies such as using water-sensitive isocyanates,<sup>21</sup> creating self-healing coatings by the precipitation of hydrogen-bonded tannic acid-poly(ethylene glycol) complexes in aqueous solution,<sup>22</sup> seawater-triggered dynamic coordination–dissociation behavior,<sup>23</sup> water-enabled interfacial hydrogen bonding,<sup>24</sup> or swelling and softening the material in water<sup>25–27</sup> have been used to produce water-triggered self-healing materials. As water-sensitive B–O bonds<sup>28</sup> enable a reversible equilibrium switch between boroxine and boronic acid to achieve dynamic cross-linking,<sup>29</sup> boroxine has acquired a lot of attention in recent years as a reversible cross-linker triggered by water.<sup>30,31</sup> For instance, researchers have cross-linked boroxine with poly(dimethylsiloxane) (PDMS),<sup>32</sup> poly(propylene glycol),<sup>33</sup> and poly(acrylic acid)<sup>34</sup> to obtain self-healable materials with variable properties under different healing conditions. However, to achieve a very stiff yet self-

Received: March 8, 2019

Accepted: April 18, 2019

Published: April 18, 2019

healable polymer-boroxine system is still challenging because the limited chain mobility of stiff polymers restricts the diffusion of the polymer chains along polymer–polymer interfaces in an opposite way to enable self-healing functionality.<sup>35</sup> In other words, it is still challenging to achieve a modulus as high as 1 GPa (common for thermoset epoxy) in self-healing polymer systems, although increasing the cross-linking network density<sup>36</sup> or fabricating boroxine-based polymer composites<sup>34</sup> can improve mechanical properties to a certain degree. Moreover, because dynamic cross-linking networks are intrinsically weaker than permanent covalent ones, it is impossible to make dynamic networks cross-linked by 100% boroxine with mechanical performances comparable to the classical thermosets.<sup>37</sup> Self-healing and recyclable thermoset materials with superior mechanical properties are highly desirable in manufacturing coatings and adhesives, aerospace parts, and electronic devices. Therefore, exploration of strategies to fabricate self-healable thermosets with excellent mechanical performance is particularly meaningful.

Sea cucumbers can rapidly and reversibly tune the stiffness of their body when in defense, exhibiting a modulus increase by a factor of 10.<sup>38</sup> This unique property comes from their specific architecture, namely, collagen fibrils cross-link in response to an external stimulus, tuning the body from a soft state (permanent matrix control) to a stiff state (cross-linked collagen fibrils penetrating the permanent matrix control).<sup>39</sup> Vice versa, this stiff structure can return to the initial soft one when the danger is gone. Inspired by this, we envision developing a new dynamic polymer system with a combination of permanent and reversible networks obtained by cross-linking poly(propylene glycol) (PPG) with boroxine and epoxy to form a hybrid system containing both reversible and permanent covalent bonds. We must emphasize that both networks are compatible in terms of reaction pathways, making the tuning of their performance easy. The reversibility of the boroxine bonds endows the self-healing functionality, while the permanent epoxy network interconnected by the boroxine links renders the system superior mechanical properties comparable with classical epoxy thermosets. This material can change properties from a stiff thermoset to an ultrasoft rubber by water stimulus with around 150 times modulus change (never reported in literature) due to the microstructure change in the mixed network. Unlike classical epoxy thermosets, which are only one-time, shapeable during curing, this system can be shaped and patterned multiple times, thus saving materials and energy in manufacturing. Such hybrid epoxy-boroxine networks have potential applications in transfer printing, nanoelectrode lithography, and with the incorporation of conductive nanofillers in versatile self-healable conductors/sensors that we highlight in this contribution.

## 2. EXPERIMENTAL SECTION

**2.1. Materials.** Epoxy resin diglycidyl ether of bisphenol A (DGEBA), poly(propylene glycol)bis(2-aminopropyl ether) (PPG) with an average  $M_n$  value of  $\sim 400$ , and poly(caprolactone) (PCL) with an average  $M_n$  value of  $\sim 80,000$  were purchased from Sigma-Aldrich. 2-Formylphenylboronic acid (98%) and dimethylformamide (DMF, 99.8%) were purchased from Acros Organics. Poly(dimethylsiloxane) (PDMS, Sylgard 184) was purchased from Dow Corning Corp. Branched carbon nanotubes (CNS), known as carbon nanostructures (flake 70  $\mu\text{m}$  long, 10  $\mu\text{m}$  thick, and about 9 nm nanotube in diameters), were provided by Applied Nanostructured Solutions LLC (Lockheed Martin Corporation, MD, US). Commercial acrylic adhesive (Lord 204) was purchased from Lord Corp.

**2.2. Sample Preparation and Characterization.** **2.2.1. Epoxy-Boroxine Preparation.** 2-Formylphenylboronic acid was first dried under vacuum at 70 °C for 8 h to form boroxine through dehydration. PPG was dissolved in DMF before being mixed with a stoichiometric amount of DGEBA and boroxine to form a clear solution (molar ratio of PPG/DGEBA is 1:2, molar ratio of PPG/boroxine is 3:2). The properties of the networks could be readily tuned by the molar ratio of boroxine/DGEBA, keeping the ratio of  $\text{NH}_2/(\text{epoxy} + \text{aldehyde})$  equal to 1. The ratio of boroxine/DGEBA was selected as 1:1, 3:2, 2:1, and 3:1. Then, the solution was casted on a Teflon mold and reacted at 80 °C for 12 h. The residual solvent in the cured samples was fully removed by drying under vacuum at 80 °C for another 24 h, as confirmed by thermogravimetric analysis (TGA) of cured epoxy-boroxine shown in Figure S3b.

**2.2.2. CNS-Epoxy-Boroxine Nanocomposites Preparation.** A fixed mass ratio of 0.75 wt % CNS to the total amount of epoxy-boroxine was first dispersed in DMF by ultrasonication for 10 min (cycle time of 10 s, duty cycle of 50%, amplitude of 30%, and power of 750 W). Then, PPG, DGEBA, and boroxine were added to the solution in sequence, and magnetic stirring was applied until they were fully dissolved. Next, the solution was casted on a Teflon mold and reacted at 80 °C for 12 h, followed by drying under vacuum at 80 °C for another 24 h to remove the solvent.

**2.2.3. Pattern and Erase Epoxy-Boroxine Films.** An epoxy-boroxine film with a thickness of 2 mm was first immersed in water for 2 days changing from a stiff to soft stretchable state, followed by compression to a patterned substrate under a 10 N pressure at 80 °C for 12 h. A stiff and strong epoxy-boroxine can be obtained upon heating. Re-immersing the patterned epoxy-boroxine in water for 2 days can erase the pattern.

**2.2.4. Pattern Transfer.** PDMS was prepared by first mixing the base and curing agent in a ratio of 10:1 at room temperature for several minutes. Then, the mixture was poured into a glass petri dish paved with a patterned epoxy-boroxine film cured for 24 h at room temperature. PCL with an  $M_n$  value of  $\sim 80,000$  was degassed and melted at 80 °C then covered by a patterned epoxy-boroxine film and cooled down at room temperature for crystallization.

**2.2.5. Mechanical Characterization.** Uniaxial tensile tests were performed at room temperature using a Zwick Roell tensile machine (mode Z0.5). At least five rectangular specimens  $304.0 \times 0.8 \text{ mm}^3$  (length  $\times$  width  $\times$  thickness) were tested with a loading rate of 5 mm/min.

Single-lap shear experiments were performed at room temperature with a MTS universal tensile tester (model 2525-806, MTS System Corporation, MN, USA). Lap shear testing was used to evaluate the adhesion strength of epoxy-boroxine on the aluminum substrate ( $150 \times 25 \times 1.5 \text{ mm}^3$ ). Aluminum plates were sanded with 50 grit sandpaper and rinsed with acetone. Two grams of epoxy-boroxine-PPG mixture was dissolved in 1 mL of DMF, then 250 mg of the solution was applied to the aluminum substrate to form the overlapping ( $12.5 \times 25 \text{ mm}^2$ ), next cured at 80 °C for 12 h and dried under vacuum at 80 °C for 24 h. Tests were performed with a loading rate of 2 mm/min.

**2.2.6. Thermal and Thermal Mechanical Analyses.** Glass transition temperature  $T_g$  values of the epoxy and epoxy-boroxine were measured by differential scanning calorimetry (DSC) on a TA Instruments Q100 DSC. Samples were ramped from an equilibrium temperature of  $-80$  to 100 °C at a heating rate of 5 °C/min.

Dynamic mechanical properties were characterized by a TA Q800 dynamic mechanical analyzer (DMA) in tension mode. Samples were cut in a rectangular shape with dimensions of  $30 \times 4.7 \times 1 \text{ mm}^3$ . Samples were loaded at 0.05% constant strain ramped from  $-80$  to 100 °C at a heating rate of 2 °C/min with a frequency of 1 Hz.

Thermogravimetric analysis (TGA, Q500, TA Instruments) was used to measure the amount of residual solvent in the system. Samples with a weight of  $\sim 10$  mg were heated from room temperature to 500 °C with a heating rate of 10 °C/min in an air atmosphere (flow rate of 50 mL/min).

**2.2.7. Microscopy and Spectroscopy Characterization.** Scanning electron microscopy (SEM, Nova NanoLab 200) was used to observe

the CNS dispersion in epoxy-boroxine and the healed scar of epoxy-boroxine tensile sample after an 8-h healing at 80 °C. The sample was coated with gold before SEM analysis.

Morphology of as-received CNS was analyzed by an FEI Tecnai F30 transmission electronic microscope (TEM). Before analysis, the filler was dispersed in DMF by ultrasonication.

The dispersion of CNS in epoxy-boroxine was observed by an optical microscope equipped with a camera (Olympus BX51TF, Tokyo, Japan). Before analysis, the nanocomposite samples were cut into thin sections (3  $\mu\text{m}$  in thickness) using a microtome (Leica EM FC6) at  $-80$  °C with the aid of liquid  $\text{N}_2$ .

Digilab FTS 7000 ATR rapid scan spectrometer in transmittance mode was used for Fourier transform infrared spectroscopy (FTIR) characterization.

**2.2.8. Piezoresistive Behavior.** Room-temperature electrical resistance of CNS-epoxy-boroxine nanocomposites was measured using a resistance set (PRS-801, Prostat Corporation). Piezoresistive behavior of the wet samples was investigated by recording their electrical resistances (Keithley multimeter 2701) during the tensile testing (Zwick Roell Z0.5, Germany) at room temperature. Resistance of the dry sample was recorded by the same multimeter during the cyclic tensile test in the same tensile machine under a maximum stress of 20 MPa to mimic the force change in an artificial Achilles tendon during movement.

### 3. RESULTS AND DISCUSSION

**3.1. Synthesis of Epoxy-Boroxine Network.** Sea cucumbers can rapidly and reversibly alter their stiffness from soft to stiff due to the cross-linking and decross-linking of collagen fibrils in a low-modulus matrix (see Figure 1a). Inspired by biologically self-healable and mechanically adaptive hierarchical network structures in the sea cucumbers, dynamic covalent boroxine bonds and permanent epoxy bonds were used to cross-link PPG chains into a three-dimensional (3D)

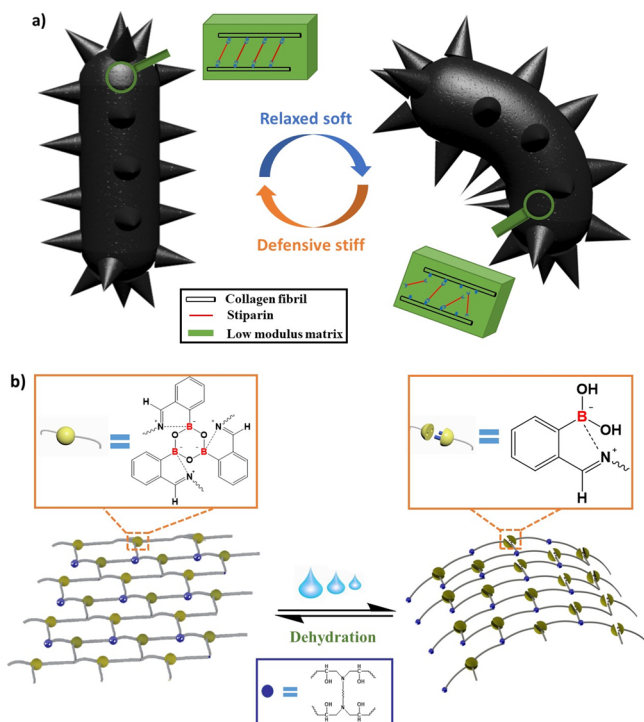


**Figure 1.** (a) Structure change and property tunable process in the sea cucumber. (b) Mechanism of water-triggered self-healing and property tunable process for epoxy-boroxine hybrid network structure. The blue beads represent the epoxy permanent cross-links.

network. The boroxine ring contains water-sensitive B–O bonds, which enable the reversible equilibrium switch between boroxine and boronic acid to achieve dynamic cross-linking as extensively reported in literature.<sup>33,34,36</sup> The cross-linked epoxy-boroxine network is stiff and strong in the dry state when both dynamic covalent and permanent bonds coexist. Upon water contact, the boroxine bonds dissociate to form free boronic acid, thus breaking the dynamic network. As such, only the epoxy permanent network conveys the mechanical strength, and the system behaves like a soft rubber. Once water is removed, boronic acid can reverse back to boroxine, providing the system self-healing functionality and returning to its original stiffness. Figure 1b illustrates the mechanism of reversible network structure change with/without water stimuli, governing the self-healing and property switch process in the epoxy-boroxine system.

Epoxy-boroxine systems with a series of ratios of epoxy to boroxine, that is, 1:1, 1:2, 1:3, and 2:3 based on molar amount of consumed PPG, were prepared, and the presence of boron-based rings of boroxine in the system was proved by Fourier transform infrared (FTIR) spectra, as shown in Figure S1 in the Supporting Information. The bands at 740 and 692  $\text{cm}^{-1}$  are attributed to the characteristic peaks of boroxine,<sup>32</sup> as seen in Figure S1b. The band at 1635  $\text{cm}^{-1}$  is assigned to the imine band ( $-\text{C}=\text{N}$  stretching) (see Figure S1a), confirming the formation of iminoboronate-based boroxine due to the reaction between  $\text{NH}_2\text{-PPG-NH}_2$  and boroxine.<sup>33</sup> Besides, the intensity of these characteristic peaks increases with an increasing ratio of boroxine to epoxy, indicating forming higher degree of dynamic bonding (FTIR curves were normalized by the C–O stretching band at 1090  $\text{cm}^{-1}$ ). Dynamic mechanical analysis (DMA) in Figure S2a reveals that the room-temperature modulus of the polymer system increases with increasing the amount of permanent bonds. However, as stiffness restricts molecular chain diffusion along the polymer interface, very stiff polymer materials are not preferred for efficient self-healing.<sup>40</sup> To balance the mechanical properties and self-healing performance, epoxy-boroxine with a ratio of 2:3 was chosen in this study. Glass-transition temperature ( $T_g$ ) of the polymer system was characterized by both DMA and differential scanning calorimetry (DSC). Measurement results in Figures S2b and S3a show that the  $T_g$  of epoxy cross-linked PPG is about 40 °C and PPG cross-linked by epoxy-boroxine with a ratio of 2:3 is 33 °C.

**3.2. Mechanical Properties and Self-Healing Ability of Epoxy-Boroxine System.** Figure 2a presents the tensile properties of epoxy-boroxine system, and the detailed results are summarized in Table S1. This epoxy system has a Young's modulus and tensile stress of  $1059 \pm 72$  and  $37.23 \pm 2.79$  MPa, respectively, on par with classical epoxy thermosets<sup>41</sup> and other high performance malleable epoxies<sup>42,43</sup> and so far are the highest values reported in literature for boroxine-based self-healing polymers.<sup>32–34</sup> They are also stiffer than most other self-healing polymer systems.<sup>44</sup> Such high modulus and tensile stress are due to the interlocking between the epoxy permanent network, and the boroxine cross-linking units creating double cross-linked networks in the system. To compare the cross-linked network of the neat epoxy with the epoxy-boroxine system, swelling tests were done by immersing a rectangular epoxy and epoxy-boroxine pieces into DMF for 24 h, and the specimen weights were measured before and after swelling. The degree of swelling (DS) was defined by the following equation<sup>45</sup>



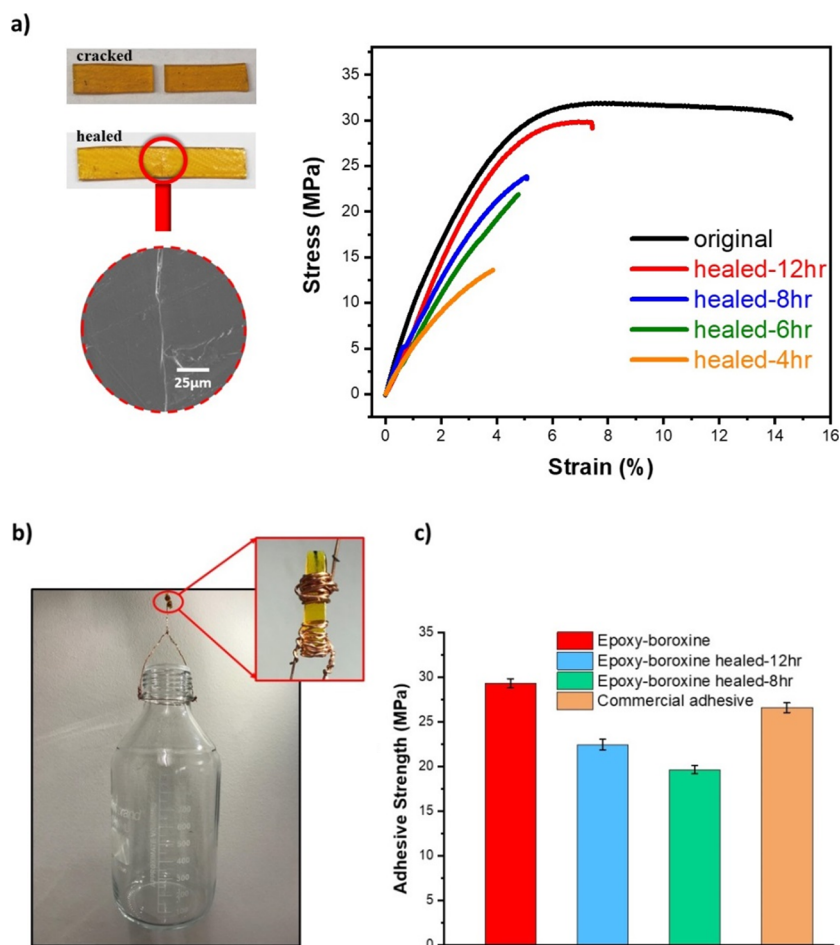


**Figure 2.** (a) SEM image of a tensile sample healed at 80 °C for 8 h and stress–strain curve of the original and healed epoxy-boroxine with different healing times. (b) Picture showing that a healed epoxy-boroxine strip film (45 mg) withstands a weight of 580 g. (c) Adhesion strength of the original and healed epoxy-boroxine systems vs a commercial adhesive applied on the aluminum substrate.

$$DS = (W_w - W_d) / W_d \times 100\% \quad (1)$$

where  $W_w$  and  $W_d$  are the weights after and before swelling, respectively. As shown in Table S2, the DS of neat epoxy is 78%, while that for the epoxy-boroxine system is 101%, indicating the latter has a slightly lower cross-linking density than the neat epoxy. However, this difference is not too big, allowing for mechanical performance at par with classical epoxy.

To observe the water-responsive self-healing behavior, rectangular samples were cut into two pieces by razor blade, and the cut surfaces were exposed to water for 10 min. The wet surfaces brought in contact were healed at 80 °C under pressure for different times. The temperature (80 °C) was selected as the healing temperature for the reversible reaction based on kinetic studies reported in literature.<sup>36</sup> The healing of the cracked sample after 8 h under appropriate pressure at 80 °C looks almost complete, as shown in the photo in Figure 2a, and was also verified by the scanning electron microscopy (SEM) image under the photo. Tensile testing was performed on the healed samples to further demonstrate the self-healing properties. As shown in Figure 2a and Table S1, with increasing healing time, the system recovers its original properties to different degrees. Twelve-hour healing renders 82.76 and 79.46% recovery of the Young's modulus and tensile strength, respectively, but only 49% of the elongation at break, most likely due to damage of parts of the epoxy permanent

network. Although 100% healing efficiency was not obtained, a Young's modulus of 773 MPa and a tensile strength of 28 MPa are still higher than most literature reported values for other self-healing polymer-boroxine systems.<sup>32–34,36</sup> Good recovery of the mechanical properties can be ascribed to the reversibility of the network, in which boronic acid can reverse back to boroxine once water is removed thus returning to its original stiffness as shown in Figure 1b. The reversibility of the boroxine bonds was also proved by FTIR as shown in Figure S4 and will be discussed later. Moreover, a 44 mg (width, 0.25 cm × thickness, 0.2 cm) healed epoxy-boroxine film is able to hold a weight of 580 g, namely, 13,000 times of its own weight, withstanding 1.14 MPa as shown in Figure 2b, indicating a high healing quality and potential for lightweight but stiff structure material applications. To check the stability of these materials at ambient temperature and humidity, specimens exposed for 2 weeks to different humidity conditions (33, 65, and 85% RH at room temperature) were tested under the same tensile testing conditions. Results shown in Figure S5 and Table S3 indicate that this material is relatively stable under ambient conditions (65% RH), as the Young's modulus and tensile stress remain as high as 810 and 23.8 MPa, respectively. Most likely, epoxy hydrophobicity prevents air humidity penetration through the network to break the boroxine bonds.

This system may have potential application as healable adhesives as demonstrated by the results of single-lap shear test

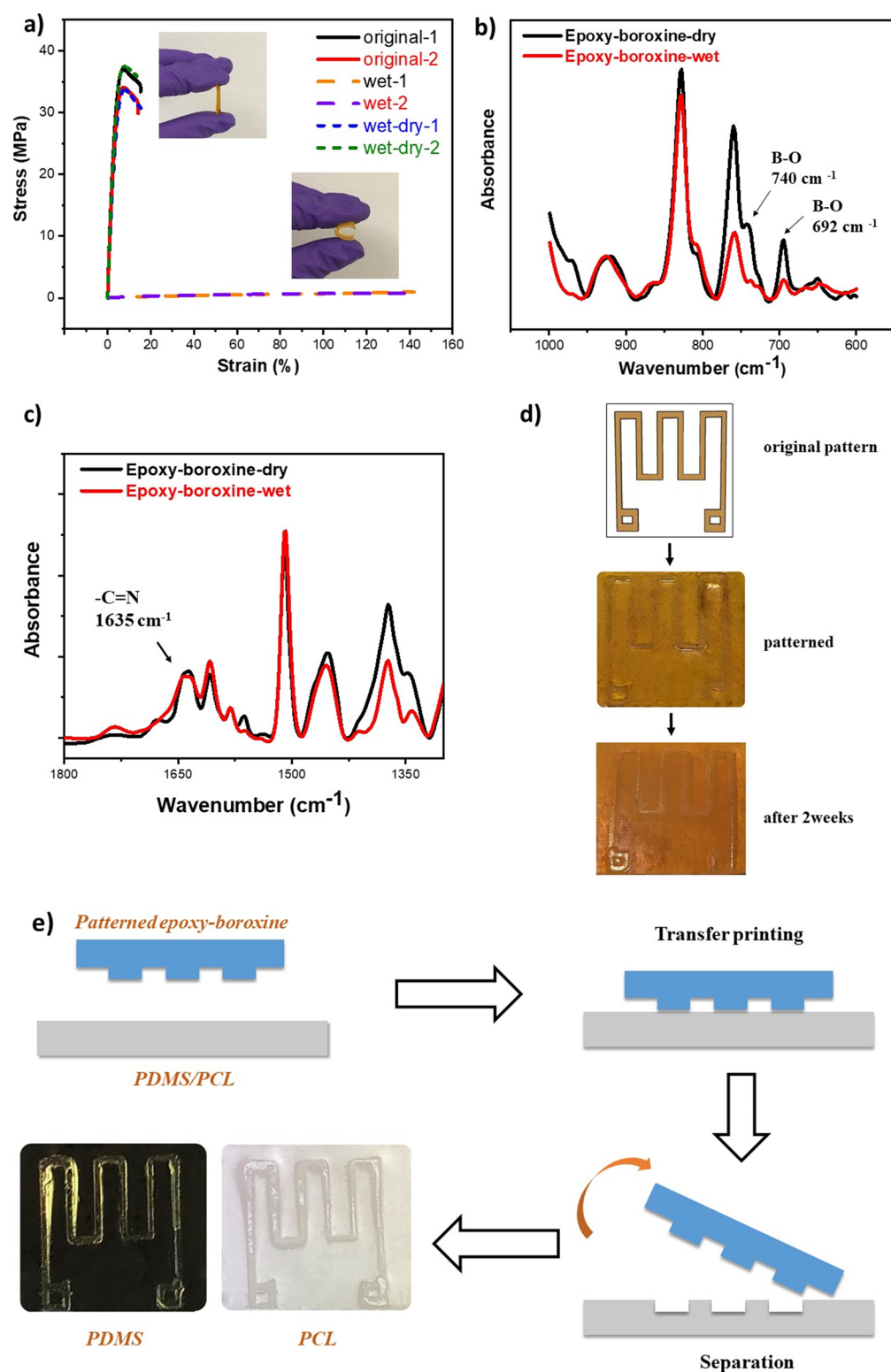


**Figure 3.** (a) Stress–strain curves of original dry, wet, and dried after wet epoxy-boroxine system, and the insets showing the softness change of the system at two states. FTIR spectra of dry and wet epoxy-boroxine system (b) between 1000 and 600  $\text{cm}^{-1}$  wavenumber, showing the reversibility of the boroxine bond, and (c) between 1800 and 1200  $\text{cm}^{-1}$  wavenumber, showing the stability against water of the iminoboronate bond. (d) Epoxy-boroxine patterned with a dummy strain gauge, after 2 weeks exposed to ambient humidity, and (e) strain gauge pattern transfer on PDMS and PCL.

on the aluminum substrate. As shown in Figure 2c, the adhesion strength of epoxy-boroxine cured at 80  $^{\circ}\text{C}$  reaches 30 MPa, which is even higher than that of a commercial structural adhesive (27 MPa) cured under similar conditions. Such

strong adhesion<sup>46</sup> may be due to the strong interactions between the epoxy-boroxine and aluminum substrate<sup>47,48</sup> and the high toughness of epoxy-boroxine.<sup>49</sup> More interestingly, the adhesion strength of this adhesive reaches 22.5 MPa after a

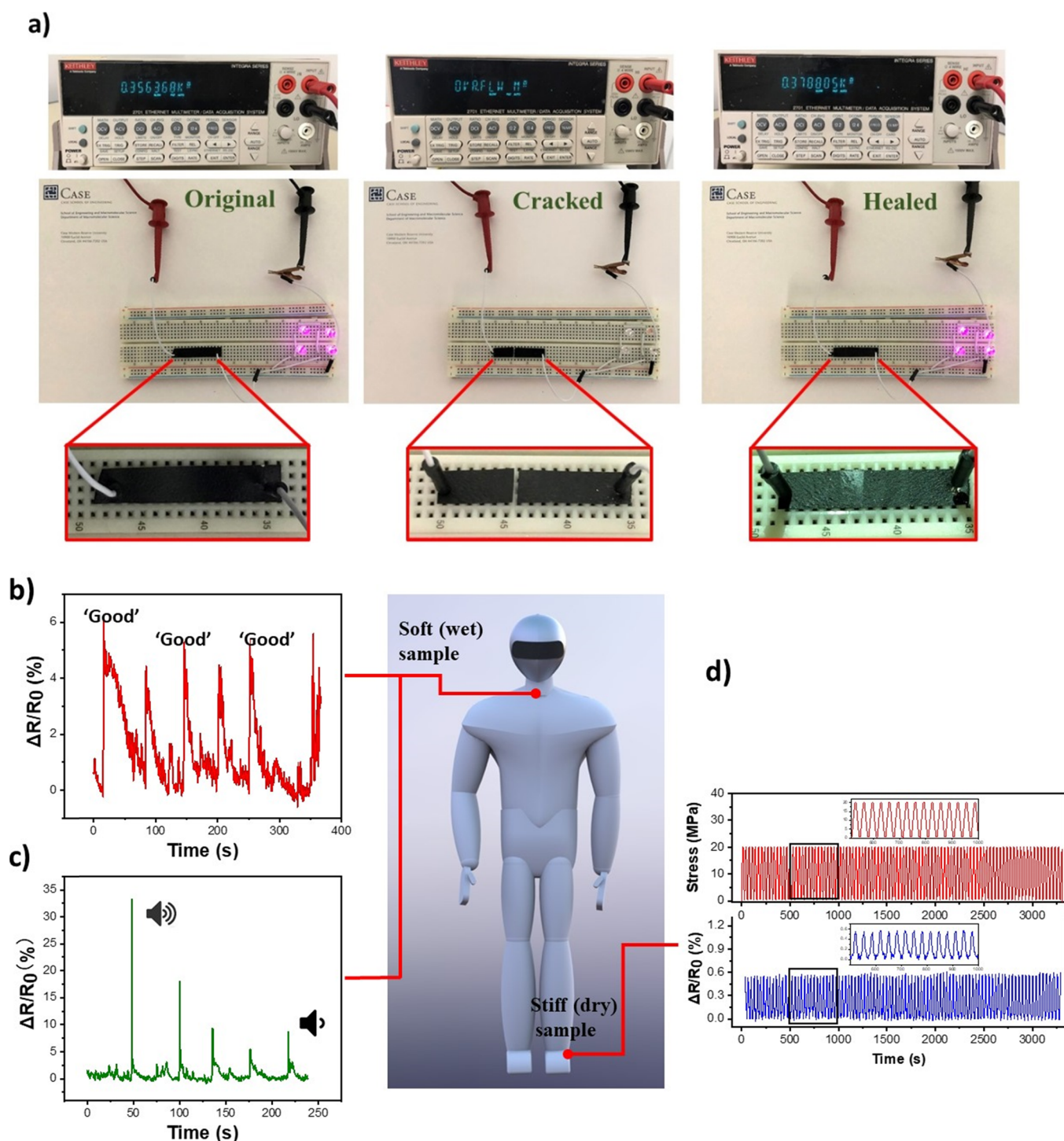


**Figure 4.** (a) Epoxy-boroxine system with CNS was used as a resistor connected to a LED bulb circuit to check the lamp lighting at three states: before damage, cracked, and healed. Relative resistance change ( $\Delta R/R_0$ ) of the wet (soft) sample plotted with time for monitoring the larynx muscle movement during (b) repeating speech and (c) speech at different volumes. (d)  $\Delta R/R_0$  plotted with time for the dry (stiff) sample under hundreds of tensile cycles with a maximum stress of 20 MPa to mimic the force change in an Achilles tendon during movement.

12-h healing at 80 °C if reused after damage, indicating the potential for manufacturing reusable epoxy-based adhesives.

### 3.3. Epoxy-Boroxine System with Tunable Properties.

Moreover, this material can change properties from an ultrasoft rubber to a stiff thermoset upon dehydration and back, once subjected to water wetting. Tensile test results of the dry and wet samples (after exposing to water for 48 h) are shown in Figure 3a and Table S4. Young's modulus and tensile strength

of the wet epoxy-boroxine are 6.77 and 0.78 MPa, which is 156 and 47 times lower than the dry epoxy-boroxine, respectively. However, the elongation at break of the wet sample is 7.2 times higher than the dry one, indicating a transition from a strong and stiff thermoset to an ultrasoft rubber after water wetting. In turn, the material returns to its original mechanical properties after removing water and can be softened again upon water treatment as shown in Table S4. To prove the property change



resulted from the breakage of the dynamic boroxine bonds, FTIR was used to check the characteristic peak of boroxine in the dry and wet states. As shown in Figure 3b, the intensity of the bands at 740 and 692  $\text{cm}^{-1}$  decreased on the wet sample by comparison with the dry one, indicating a reduced number of boroxine bonds upon wetting (FTIR curves were normalized by C–O stretching band at 1090  $\text{cm}^{-1}$ ). FTIR data of the re-dried sample indicate the recovery of boroxine characteristic peaks as shown in Figure S5. Further water treatment reduces the boroxine characteristic peaks, again confirming the excellent reversibility of the boroxine bond to water in the epoxy compound. Although classical imines can also be hydrolyzed,<sup>50,51</sup> in this system, nitrogen-coordinated imine is formed (i.e., iminoboronate specie), due to the  $=\text{N}\rightarrow\text{B}$  coordinating bond as shown in Figure 1b, which is much less hydrolyzable.<sup>33,52</sup> The FTIR results of dry and wet samples (Figure 3c) suggest that the intensity of the imine bonds at 1635  $\text{cm}^{-1}$  keeps almost the same upon water treatment, indicating its low sensitivity to water. Therefore, the switch between boroxine and boronic acid dominates the healing and network reversibility in this system. In addition, swelling test results in Table S5 show that there is no weight loss upon drying after swelling, indicating that tethered boronic acid chains are present in the network to reform boroxine bonds upon water removal rather than being washed out after decross-linking. This accounts for the 100% recovery of the mechanical properties after drying. Therefore, this system is capable of switching from a stiff network to an ultrasoft one upon water contact, broadening the potential applications of this self-healing polymer system for different functional materials. Although other smart polymeric materials with switchable mechanical properties were reported in literature,<sup>53–55</sup> such a wide range of property change at room temperature for a nonfiller reinforced polymer has been rarely seen. This feature can expand the application range of such systems to pattern printing and flexible electronics.

Figure 3d shows that this material can easily print the patterns from a dummy strain gauge while in the wet stage, and the patterns remain engraved upon drying. More importantly, these patterns hold for more than 2 weeks in ambient conditions but can be easily erased by an appropriate water treatment thus enabling applications for micro/nanofabrication of epoxy-based materials. In addition, as shown in Figure 3e, the epoxy-boroxine system is also suitable for transfer printing applications due to the stiff nature of the material in the dry stage. The dummy strain gauge pattern can be successfully transferred from epoxy-boroxine to PDMS and PCL. The well-patterned PDMS can be widely used in the field of pattern transfer,<sup>56</sup> micro/nanofluidics,<sup>57</sup> and electrical insulation,<sup>58</sup> while patterning PCL is applicable in biomedical applications such as tissue engineering.<sup>59</sup> Such epoxy-boroxine systems can be used as versatile, functional materials for transfer printing in the micro/nanofabrication of smart materials.<sup>60</sup>

**3.4. CNS-Epoxy-Boroxine Nanocomposites for Wearable Sensors.** Moreover, the incorporation of fillers may potentially expand the range of applications for these systems. One example is the addition of conductive fillers to tailor the properties toward applications such as self-healing conductors/resistors or elastomer-based sensors.<sup>61–63</sup> In this work, branched carbon nanotubes, known as carbon nanostructures (CNS) (Figure S6), were incorporated in the epoxy-boroxine system. CNS tree-like morphology favors the interconnection of the branches to form an effective pathway for conductive

network.<sup>64</sup> The epoxy-boroxine system with 0.75 wt % CNS shows a good filler dispersion (Figures S7 and S8) and has an electrical conductivity of 23 S/m. Figure 4a demonstrates that the electrical resistance of a cut specimen can return to the original one upon healing, as evidenced by the brightness of the LED bulbs and the resistance reading in the Keithley digital multimeter. Therefore, such systems can be used as epoxy-based self-healing conductive composite materials in conductors or resistors.

Besides, this composite can be used as strain sensors for detecting human body motion.<sup>65,66</sup> For instance, the softness of the wet CNS-epoxy-boroxine allows its use as wearable strain sensor to monitor the muscle motion in the larynx during oration.<sup>67</sup> Reproducible signals of the same speech and the pronunciation of a word at different volumes can be clearly marked, as seen in Figure 4b,c. This system is comparable with elastomer-based conductive composites used in wearable sensors.<sup>68–70</sup> Furthermore, this material is self-healable, which may broaden its application in electronics, for self-healing flexible sensors. On the other hand, the high stiffness of the dry CNS-epoxy-boroxine makes it suitable for detecting the stress in prosthetic limbs or cracked bones in recovery, to assist healthcare for patients during walking and jogging. As an example, considering the mechanical properties of the human Achilles tendon (816  $\pm$  218 MPa modulus, 71  $\pm$  17 MPa failure stress, and 12.8  $\pm$  1.7% failure strain),<sup>71</sup> the dry CNS-epoxy-boroxine system may be adequate to detect the force generated on an Achilles tendon during exercise.<sup>72</sup> Hundreds of tensile cycles with a maximum stress of 20 MPa were applied on the dry CNS-epoxy-boroxine sample, and the results are shown in Figure 4d. The reproducible signals of resistance change  $\Delta R/R_0$  versus time during the loading and unloading indicate the reliability of this material for the body motion monitoring targeted at a large stress detection. To evaluate the strain sensitivity, the gauge factor ( $G_F$ ) values of dry and wet CNS-epoxy-boroxine samples calculated based on a linear fitting of  $\Delta R/R_0$  versus strain are provided in Figure S9. The wet sample has a  $G_F$  value of 3.2 for strain 3–18%, higher than the dry one with a  $G_F$  value of 2.1, due to the soft nature of the polymer matrix. Besides, the  $G_F$  value for higher-level strains (e.g., strain between 55 and 72%) is up to 15.3, as seen in Figure S9. The measured  $G_F$  values are comparable with literature reported  $G_F$  values (2–16) for epoxy-multi-walled carbon nanotube conductive sensors.<sup>73</sup> This is the first report on a polymer-based material with tunable stiffness toward self-healing electronic applications.

## 4. CONCLUSIONS

In summary, inspired by the sea cucumber, we have designed a water-responsive self-healing polymer system with reversible and permanent covalent cross-linking networks by cross-linking poly(propylene glycol) with boroxine and epoxy. This system has mechanical properties at a par with classic epoxy thermosets while also showing self-healing ability upon wetting due to the disassociation of dynamic boroxine bonds with up to 80% recovery of modulus and mechanical strength after healing. The epoxy-boroxine system is much more stable in ambient conditions by comparison with other boroxine-based self-healing systems due to the hydrophobicity nature of epoxy. This system is suitable for applications in self-healable structural adhesives with properties comparable to commercial adhesives. Moreover, the mechanical properties can be reversibly tuned from a stiff thermoset to soft rubber by

water stimulus with potential applications in direct and transfer printing for microfabrication, in which patterns can be applied and erased facily on target substrates. By adding CNS into the system, we obtained healable piezoresistive sensors with tunable properties and demonstrated potential applications in monitoring different body motions from larynx to limb movements.

## ■ ASSOCIATED CONTENT

### 📄 Supporting Information

The Supporting Information is available free of charge on the ACS Publications website at DOI: 10.1021/acsami.9b04249.

FTIR, DMA of epoxy-boroxine system, and DSC curves of epoxy and epoxy-boroxine; TGA of cured epoxy-boroxine; tensile properties of original and healed epoxy-boroxine; swelling test of epoxy and epoxy-boroxine in DMF and water; FTIR and tensile properties of epoxy-boroxine under two wet-dry cycles; representative stress–strain curve of original epoxy-boroxine and epoxy-boroxine exposed to different humidity conditions for two weeks; tensile properties of original epoxy-boroxine and epoxy-boroxine exposed to ambient humidity for two weeks; TEM of CNS; OPM of epoxy-boroxine with CNS; and linear fitting of relative resistance change ( $\Delta R/R_0$ ) versus strain for CNS-epoxy-boroxine samples (PDF)

## ■ AUTHOR INFORMATION

### Corresponding Authors

\*E-mail: kxk424@case.edu (K.K.).

\*E-mail: jean-marie.raquez@umons.ac.be (J.-M.R.).

\*E-mail: ixm@case.edu (I.M.-Z.).

### ORCID

Dian Yuan: 0000-0002-8699-4127

Kai Ke: 0000-0002-6283-0689

Jean-Marie Raquez: 0000-0003-1940-7129

### Notes

The authors declare no competing financial interest.

## ■ ACKNOWLEDGMENTS

The authors gratefully acknowledge the National Science Foundation for the financial support of this research through grant PIRE 1243313. We also appreciate the Applied Nanostructured Solutions LLC for providing CNS for our research. We give special thanks to Jinghao Yang, Bertrand Willocq, and Zhen Sang for their assistance in this study. J.-M.R. is a FRS-FNRS research fellow.

## ■ REFERENCES

- (1) Wool, R. P. Self-Healing Materials: A Review. *Soft Matter* **2008**, *4*, 400–418.
- (2) Wu, D. Y.; Meure, S.; Solomon, D. Self-Healing Polymeric Materials: A Review of Recent Developments. *Prog. Polym. Sci.* **2008**, *33*, 479–522.
- (3) Cho, S. H.; White, S. R.; Braun, P. V. Self-Healing Polymer Coatings. *Adv. Mater.* **2009**, *21*, 645–649.
- (4) Hamilton, A. R.; Sottos, N. R.; White, S. R. Self-Healing of Internal Damage in Synthetic Vascular Materials. *Adv. Mater.* **2010**, *22*, 5159–5163.
- (5) Lee, M. W.; An, S.; Lee, C.; Liou, M.; Yarin, A. L.; Yoon, S. S. Self-Healing Transparent Core–shell Nanofiber Coatings for Anti-Corrosive Protection. *J. Mater. Chem. A* **2014**, *2*, 7045–7053.

- (6) Yuan, D.; Bonab, V. S.; Patel, A.; Manas-Zloczower, I. Self-Healing Epoxy Coatings with Enhanced Properties and Facile Processability. *Polymer* **2018**, *147*, 196–201.

- (7) Imato, K.; Nishihara, M.; Kanehara, T.; Amamoto, Y.; Takahara, A.; Otsuka, H. Self-Healing of Chemical Gels Cross-Linked by Diarylbibenzofuranone-Based Trigger-Free Dynamic Covalent Bonds at Room Temperature. *Angew. Chem., Int. Ed.* **2012**, *51*, 1138–1142.

- (8) Ying, H.; Zhang, Y.; Cheng, J. Dynamic Urea Bond for the Design of Reversible and Self-Healing Polymers. *Nat. Commun.* **2014**, *5*, 3218.

- (9) Amamoto, Y.; Otsuka, H.; Takahara, A.; Matyjaszewski, K. Self-Healing of Covalently Cross-Linked Polymers by Reshuffling Thiuram Disulfide Moieties in Air under Visible Light. *Adv. Mater.* **2012**, *24*, 3975–3980.

- (10) Holten-Andersen, N.; Harrington, M. J.; Birkedal, H.; Lee, B. P.; Messersmith, P. B.; Lee, K. Y. C.; Waite, J. H. PH-Induced Metal-Ligand Cross-Links Inspired by Mussel Yield Self-Healing Polymer Networks with near-Covalent Elastic Moduli. *Proc. Natl. Acad. Sci.* **2011**, *108*, 2651–2655.

- (11) Cordier, P.; Tournilhac, F.; Soulié-Ziakovic, C.; Leibler, L. Self-Healing and Thermoreversible Rubber from Supramolecular Assembly. *Nature* **2008**, *451*, 977.

- (12) Vahedi, V.; Pasbakhsh, P.; Piao, C. S.; Seng, C. E. A Facile Method for Preparation of Self-Healing Epoxy Composites: Using Electrospun Nanofibers as Microchannels. *J. Mater. Chem. A* **2015**, *3*, 16005–16012.

- (13) Hia, I. L.; Chan, E.-S.; Chai, S.-P.; Pasbakhsh, P. A Novel Repeated Self-Healing Epoxy Composite with Alginate Multicore Microcapsules. *J. Mater. Chem. A* **2018**, *6*, 8470–8478.

- (14) Canadell, J.; Goossens, H.; Klumperman, B. Self-Healing Materials Based on Disulfide Links. *Macromolecules* **2011**, *44*, 2536–2541.

- (15) Hillewaere, X. K. D.; Du Prez, F. E. Fifteen Chemistries for Autonomous External Self-Healing Polymers and Composites. *Prog. Polym. Sci.* **2015**, *49-50*, 121–153.

- (16) Hernández, M.; Grande, A. M.; Dierkes, W.; Bijleveld, J.; van der Zwaag, S.; García, S. J. Turning Vulcanized Natural Rubber into a Self-Healing Polymer: Effect of the Disulfide/Polysulfide Ratio. *ACS Sustainable Chem. Eng.* **2016**, *4*, 5776–5784.

- (17) Lu, Y.-X.; Tournilhac, F.; Leibler, L.; Guan, Z. Making Insoluble Polymer Networks Malleable via Olefin Metathesis. *J. Am. Chem. Soc.* **2012**, *134*, 8424–8427.

- (18) Keller, M. W.; White, S. R.; Sottos, N. R. A Self-Healing Poly(Dimethyl Siloxane) Elastomer. *Adv. Funct. Mater.* **2007**, *17*, 2399–2404.

- (19) Oehlenschlaeger, K. K.; Mueller, J. O.; Brandt, J.; Hilf, S.; Lederer, A.; Wilhelm, M.; Graf, R.; Coote, M. L.; Schmidt, F. G.; Barner-Kowollik, C. Adaptable Hetero Diels–Alder Networks for Fast Self-Healing under Mild Conditions. *Adv. Mater.* **2014**, *26*, 3561–3566.

- (20) Hillewaere, X. K. D.; Teixeira, R. F. A.; Nguyen, L.-T. T.; Ramos, J. A.; Rahier, H.; Du Prez, F. E. Autonomous Self-Healing of Epoxy Thermosets with Thiol-Isocyanate Chemistry. *Adv. Funct. Mater.* **2014**, *24*, 5575–5583.

- (21) Wang, W.; Xu, L.; Li, X.; Lin, Z.; Yang, Y.; An, E. Self-Healing Mechanisms of Water Triggered Smart Coating in Seawater. *J. Mater. Chem. A* **2014**, *2*, 1914–1921.

- (22) Du, Y.; Qiu, W.-Z.; Wu, Z. L.; Ren, P.-F.; Zheng, Q.; Xu, Z.-K. Water-Triggered Self-Healing Coatings of Hydrogen-Bonded Complexes for High Binding Affinity and Antioxidative Property. *Adv. Mater. Interfaces* **2016**, *3*, 1600167.

- (23) Xia, N. N.; Xiong, X. M.; Wang, J.; Rong, M. Z.; Zhang, M. Q. A Seawater Triggered Dynamic Coordinate Bond and Its Application for Underwater Self-Healing and Reclaiming of Lipophilic Polymer. *Chem. Sci.* **2016**, *7*, 2736–2742.

- (24) Ahn, B. K.; Lee, D. W.; Israelachvili, J. N.; Waite, J. H. Surface-Initiated Self-Healing of Polymers in Aqueous Media. *Nat. Mater.* **2014**, *13*, 867.



- (25) Wang, X.; Liu, F.; Zheng, X.; Sun, J. Water-Enabled Self-Healing of Polyelectrolyte Multilayer Coatings. *Angew. Chem., Int. Ed.* **2011**, *50*, 11378–11381.
- (26) Sariola, V.; Pena-Francesch, A.; Jung, H.; Çetinkaya, M.; Pacheco, C.; Sitti, M.; Demirel, M. C. Segmented Molecular Design of Self-Healing Proteinaceous Materials. *Sci. Rep.* **2015**, *5*, 13482.
- (27) Taynton, P.; Yu, K.; Shoemaker, R. K.; Jin, Y.; Qi, H. J.; Zhang, W. Heat- or Water-Driven Malleability in a Highly Recyclable Covalent Network Polymer. *Adv. Mater.* **2014**, *26*, 3938–3942.
- (28) Kim, C.; Ejima, H.; Yoshie, N. Polymers with Autonomous Self-Healing Ability and Remarkable Reprocessability under Ambient Humidity Conditions. *J. Mater. Chem. A* **2018**, *6*, 19643–19652.
- (29) Korich, A. L.; Iovine, P. M. Boroxine Chemistry and Applications: A Perspective. *Dalton Trans.* **2010**, *39*, 1423–1431.
- (30) Nishiyabu, R.; Kubo, Y.; James, T. D.; Fossey, J. S. Boronic Acid Building Blocks: Tools for Self Assembly. *Chem. Commun.* **2011**, *47*, 1124–1150.
- (31) Cash, J. J.; Kubo, T.; Bapat, A. P.; Sumerlin, B. S. Room-Temperature Self-Healing Polymers Based on Dynamic-Covalent Boronic Esters. *Macromolecules* **2015**, *48*, 2098–2106.
- (32) Lai, J.-C.; Mei, J.-F.; Jia, X.-Y.; Li, C.-H.; You, X.-Z.; Bao, Z. A Stiff and Healable Polymer Based on Dynamic-Covalent Boroxine Bonds. *Adv. Mater.* **2016**, *28*, 8277–8282.
- (33) Delpierre, S.; Willocq, B.; De Winter, J.; Dubois, P.; Gerbaux, P.; Raquez, J.-M. Dynamic Iminoboronate-Based Boroxine Chemistry for the Design of Ambient Humidity-Sensitive Self-Healing Polymers. *Chem. – Eur. J.* **2017**, *23*, 6730–6735.
- (34) Bao, C.; Jiang, Y.-J.; Zhang, H.; Lu, X.; Sun, J. Room-Temperature Self-Healing and Recyclable Tough Polymer Composites Using Nitrogen-Coordinated Boroxines. *Adv. Funct. Mater.* **2018**, *28*, 1800560.
- (35) Garcia, S. J. Effect of Polymer Architecture on the Intrinsic Self-Healing Character of Polymers. *Eur. Polym. J.* **2014**, *53*, 118–125.
- (36) Ogden, W. A.; Guan, Z. Recyclable, Strong, and Highly Malleable Thermosets Based on Boroxine Networks. *J. Am. Chem. Soc.* **2018**, *140*, 6217–6220.
- (37) Wu, J.; Cai, L.-H.; Weitz, D. A. Tough Self-Healing Elastomers by Molecular Enforced Integration of Covalent and Reversible Networks. *Adv. Mater.* **2017**, *29*, 1702616.
- (38) Capadona, J. R.; Shanmuganathan, K.; Tyler, D. J.; Rowan, S. J.; Weder, C. Stimuli-Responsive Polymer Nanocomposites Inspired by the Sea Cucumber Dermis. *Science* **2008**, *319*, 1370–1374.
- (39) Mendez, J.; Annamalai, P. K.; Eichhorn, S. J.; Rusli, R.; Rowan, S. J.; Foster, E. J.; Weder, C. Bioinspired Mechanically Adaptive Polymer Nanocomposites with Water-Activated Shape-Memory Effect. *Macromolecules* **2011**, *44*, 6827–6835.
- (40) Urban, M. W. Self-Healing Polymers. From Principles to Applications. Edited by Wolfgang H. Binder. *Angew. Chem., Int. Ed.* **2014**, *53*, 3775.
- (41) Shan, L.; Verghese, K. N. E.; Robertson, C. G.; Reifsnider, K. L. Effect of Network Structure of Epoxy DGEBA-Poly(Oxypropylene)-Diamines on Tensile Behavior. *J. Polym. Sci., Part B: Polym. Phys.* **1999**, *37*, 2815–2819.
- (42) Montarnal, D.; Capelot, M.; Tournilhac, F.; Leibler, L. Silica-Like Malleable Materials from Permanent Organic Networks. *Science* **2011**, *334*, 965–968.
- (43) Liu, W.; Schmidt, D. F.; Reynaud, E. Catalyst Selection, Creep, and Stress Relaxation in High-Performance Epoxy Vitrimers. *Ind. Eng. Chem. Res.* **2017**, *56*, 2667–2672.
- (44) Chen, Y.; Guan, Z. Multivalent Hydrogen Bonding Block Copolymers Self-Assemble into Strong and Tough Self-Healing Materials. *Chem. Commun.* **2014**, *50*, 10868–10870.
- (45) Ochi, M.; Takahashi, R.; Terauchi, A. Phase Structure and Mechanical and Adhesion Properties of Epoxy/Silica Hybrids. *Polymer* **2001**, *42*, 5151–5158.
- (46) Tang, J.; Wan, L.; Zhou, Y.; Pan, H.; Huang, F. Strong and Efficient Self-Healing Adhesives Based on Dynamic Quaternization Cross-Links. *J. Mater. Chem. A* **2017**, *5*, 21169–21177.
- (47) Kahraman, R.; Sunar, M.; Yilbas, B. Influence of Adhesive Thickness and Filler Content on the Mechanical Performance of Aluminum Single-Lap Joints Bonded with Aluminum Powder Filled Epoxy Adhesive. *J. Mater. Process. Technol.* **2008**, *205*, 183–189.
- (48) Ambrose, R. J. *Adhesion and Adhesives-Science and Technology*; Kinloch, A. J., Ed.; Chapman and Hall: New York, London, 1988.
- (49) Mostovoy, S.; Ripling, E. J. The Fracture Toughness and Stress Corrosion Cracking Characteristics of an Anhydride-Hardened Epoxy Adhesive. *J. Appl. Polym. Sci.* **1971**, *15*, 641–659.
- (50) Chao, A.; Negulescu, I.; Zhang, D. Dynamic Covalent Polymer Networks Based on Degenerative Imine Bond Exchange: Tuning the Malleability and Self-Healing Properties by Solvent. *Macromolecules* **2016**, *49*, 6277–6284.
- (51) Jin, Y.; Yu, C.; Denman, R. J.; Zhang, W. Recent Advances in Dynamic Covalent Chemistry. *Chem. Soc. Rev.* **2013**, *42*, 6634–6654.
- (52) Cal, P. M. S. D.; Vicente, J. B.; Pires, E.; Coelho, A. V.; Veiros, L. F.; Cordeiro, C.; Gois, P. M. P. Iminoboronates: A New Strategy for Reversible Protein Modification. *J. Am. Chem. Soc.* **2012**, *134*, 10299–10305.
- (53) McKee, J. R.; Hietala, S.; Seitsonen, J.; Laine, J.; Kontturi, E.; Ikkala, O. Thermoresponsive Nanocellulose Hydrogels with Tunable Mechanical Properties. *ACS Macro Lett.* **2014**, *3*, 266–270.
- (54) Cudjoe, E.; Khani, S.; Way, A. E.; Hore, M. J. A.; Maia, J.; Rowan, S. J. Biomimetic Reversible Heat-Stiffening Polymer Nanocomposites. *ACS Cent. Sci.* **2017**, *3*, 886–894.
- (55) Jorfi, M.; Roberts, M. N.; Foster, E. J.; Weder, C. Physiologically Responsive, Mechanically Adaptive Bio-Nanocomposites for Biomedical Applications. *ACS Appl. Mater. Interfaces* **2013**, *5*, 1517–1526.
- (56) Wang, J.; Xie, J.; Zong, C.; Han, X.; Ji, H.; Zhao, J.; Lu, C. Surface Treatment-Assisted Switchable Transfer Printing on Polydimethylsiloxane Films. *J. Mater. Chem. C* **2016**, *4*, 3467–3476.
- (57) Huh, D.; Mills, K. L.; Zhu, X.; Burns, M. A.; Thouless, M. D.; Takayama, S. Tuneable Elastomeric Nanochannels for Nanofluidic Manipulation. *Nat. Mater.* **2007**, *6*, 424.
- (58) Park, J.; Kim, H. S.; Han, A. Micropatterning of Poly-(Dimethylsiloxane) Using a Photoresist Lift-off Technique for Selective Electrical Insulation of Microelectrode Arrays. *J. Microeng. Microfab.* **2009**, *19*, 065016.
- (59) Tiaw, K. S.; Goh, S. W.; Hong, M.; Wang, Z.; Lan, B.; Teoh, S. H. Laser Surface Modification of Poly( $\epsilon$ -Caprolactone) (PCL) Membrane for Tissue Engineering Applications. *Biomaterials* **2005**, *26*, 763–769.
- (60) Carlson, A.; Bowen, A. M.; Huang, Y.; Nuzzo, R. G.; Rogers, J. A. Transfer Printing Techniques for Materials Assembly and Micro/Nanodevice Fabrication. *Adv. Mater.* **2012**, *24*, 5284–5318.
- (61) Cai, G.; Wang, J.; Qian, K.; Chen, J.; Li, S.; Lee, P. S. Extremely Stretchable Strain Sensors Based on Conductive Self-Healing Dynamic Cross-Links Hydrogels for Human-Motion Detection. *Adv. Sci.* **2017**, *4*, 1600190.
- (62) Nambiar, S.; Yeow, J. T. W. Conductive Polymer-Based Sensors for Biomedical Applications. *Biosens. Bioelectron.* **2011**, *26*, 1825–1832.
- (63) Wang, T.; Zhang, Y.; Liu, Q.; Cheng, W.; Wang, X.; Pan, L.; Xu, B.; Xu, H. A Self-Healable, Highly Stretchable, and Solution Processable Conductive Polymer Composite for Ultrasensitive Strain and Pressure Sensing. *Adv. Funct. Mater.* **2018**, *28*, 1705551.
- (64) Ke, K.; Solouki Bonab, V.; Yuan, D.; Manas-Zloczower, I. Piezoresistive Thermoplastic Polyurethane Nanocomposites with Carbon Nanostructures. *Carbon* **2018**, *139*, 52–58.
- (65) Zheng, Q.; Liu, X.; Xu, H.; Cheung, M.-S.; Choi, Y.-W.; Huang, H.-C.; Lei, H.-Y.; Shen, X.; Wang, Z.; Wu, Y.; Kim, S.Y.; Kim, J.-K. Sliced Graphene Foam Films for Dual-Functional Wearable Strain Sensors and Switches. *Nanoscale Horiz.* **2018**, *3*, 35–44.
- (66) Liu, X.; Lu, C.; Wu, X.; Zhang, X. Self-Healing Strain Sensors Based on Nanostructured Supramolecular Conductive Elastomers. *J. Mater. Chem. A* **2017**, *5*, 9824–9832.
- (67) Liu, X.; Tang, C.; Du, X.; Xiong, S.; Xi, S.; Liu, Y.; Shen, X.; Zheng, Q.; Wang, Z.; Wu, Y.; Horner, A.; Kim, J.-K. A Highly

Sensitive Graphene Woven Fabric Strain Sensor for Wearable Wireless Musical Instruments. *Mater. Horiz.* **2017**, *4*, 477–486.

(68) Trung, T. Q.; Lee, N.-E. Flexible and Stretchable Physical Sensor Integrated Platforms for Wearable Human-Activity Monitoring and Personal Healthcare. *Adv. Mater.* **2016**, *28*, 4338–4372.

(69) Amjadi, M.; Pichitpajongkit, A.; Lee, S.; Ryu, S.; Park, I. Highly Stretchable and Sensitive Strain Sensor Based on Silver Nanowire–Elastomer Nanocomposite. *ACS Nano* **2014**, *8*, 5154–5163.

(70) Zhang, Q.; Niu, S.; Wang, L.; Lopez, J.; Chen, S.; Cai, Y.; Du, R.; Liu, Y.; Lai, J.-C.; Liu, L.; Li, C.-H.; Yan, X.; Liu, C.; Tok, J. B.-H.; Jia, X.; Bao, Z. An Elastic Autonomous Self-Healing Capacitive Sensor Based on a Dynamic Dual Crosslinked Chemical System. *Adv. Mater.* **2018**, *30*, 1801435.

(71) Wren, T. A. L.; Yerby, S. A.; Beaupré, G. S.; Carter, D. R. Mechanical Properties of the Human Achilles Tendon. *Clin. Biomech.* **2001**, *16*, 245–251.

(72) Epro, G.; Mierau, A.; Doerner, J.; Luetkens, J. A.; Scheef, L.; Kukuk, G. M.; Boecker, H.; Maganaris, C. N.; Brüggemann, G.-P.; Karamanidis, K. The Achilles Tendon Is Mechanosensitive in Older Adults: Adaptations Following 14 Weeks versus 1.5 Years of Cyclic Strain Exercise. *J. Exp. Biol.* **2017**, *220*, 1008–1018.

(73) Sanli, A.; Müller, C.; Kanoun, O.; Elibol, C.; Wagner, M. F.-X. Piezoresistive Characterization of Multi-Walled Carbon Nanotube-Epoxy Based Flexible Strain Sensitive Films by Impedance Spectroscopy. *Compos. Sci. Technol.* **2016**, *122*, 18–26.